INVESTIGATION OF THE PRESSURE DISTRIBUTION ON CERTAIN STAR-SHAPED BODIES AT M ≈ 4

A. L. Gonor and A. I. Shvets

Zhurnal Prikladnoi Mekhaniki i Tekhnicheskoi Fiziki, No. 6, pp. 122–125, 1965

It has recently been established theoretically [1, 2] that star-shaped bodies may prove to be aerodynamically promising in the sense of reduced drag and increased performance at supersonic and hypersonic speeds. Below a description is given of the results of experiments on flow over models with surface pressure taps

The investigation was conducted in a wind tunnel at Mach number 3.85 ± 0.1 and Reynolds number $6.0 \cdot 10^6$ [l = 0.2 m).

1. Measurement technique and description of models. During the tests the flow parameters in the working section and the model surface pressures were determined as follows. The stagnation pressure was measured with four total pressure tubes, and the stream static pressure was measured via several orifice taps located on the walls of the working section.

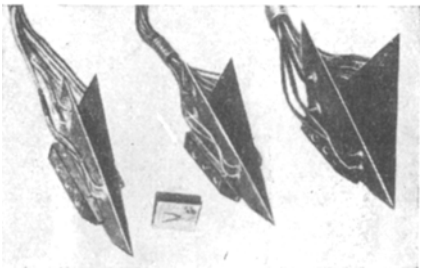

Fig. 1

In addtion, total and static pressure tubes were mounted near the model, to determine the stream parameters; these were located 20–40 mm below the model, and were extended into the free-stream region.

Model surface pressures were measured by two banks of manometers, the fluid being tetrabromoethane with specific gravity 2.96 g/cm^3. One side of each U-tube was connected to a pressure tap, while the other went to a closed volume maintained at reduced pressure during the experiment, this pressure being displayed on several tubes of a multimanometer open to the atmosphere. The total pressure behind the normal shock was measured by the drop in the level of a U-tube, also opening to the atmosphere. The duration of the test was determined by the air supply and by the time to establish the tetrabromoethane levels, and was 30–40 sec. The manometer readings were all photographed on an AFA apparatus with frame size 130 × 180 mm, which enabled the manometer banks to be read to an accuracy of ±2 mm of tetrabromoethane column. The error in measuring model pressure distribution was roughly 5%.

Three steel models with swept wings were designed for the pressure distribution tests, each model being 200 mm long; a photograph of these is shown in Fig. 1. The pressure tap scheme is shown in Fig. 2. There were 30 orifices on the model with $\pi/n = 30°$, 22 on that with $\pi/n = 18°$, and 19 on that with $\pi/n = 12°$. The orifices were located on the inner side of the wings, in two sections normal to the model axis. At places where the inside surfaces of the wings were sharply curving, the pressure taps were closer to one another, to give more accurate pressure distribution measurement in that region. The orifices were drilled normal to the wing surface and had a diameter of 0.9 mm. There were some symmetrical orifices on both sides of the wings, used for controlling the angle of bank of the model in the working section, and for checking the operation of the pressure tap system.

The model was mounted on a sting at the rear, and there was provision for translation of the model along the tunnel axis. The mounting arrangement included an angle of incidence mechanism, allowing tests in the range of angles −5° to 15°.

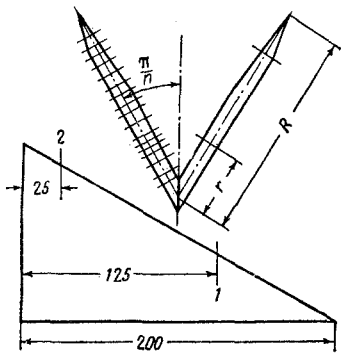

Fig. 2

All the models had identical parameters α and γ, which determine the position of the shock wave, but had substantially different values of the parameter $2\pi/n$ (the clearance angle between lobes), which varied from 24° (n = 15) to 60° (n = 6). It was proposed to elucidate in this way the influence of the boundary layer on the flow structure, since if the theory for small values of n proved to be correct, then sooner or later as n increases and the lobes approach one another, the gap between them will be filled by the boundary layer, which will promote a rearrangement of the entire flow. It was expected, in particular, that the influence of the boundary layer on the pressure distribution would be quite apparent even at n = 15.

2. **Test results and comparison with theory.** The dimensionless pressure at the model surface was determined from the formula

$$c_{p_i} = \frac{2}{\varkappa M_\infty^2}\left(\frac{p_i}{p_\infty} - 1\right),$$

where $\varkappa = 1.4$, M_∞ is the Mach number of the oncoming stream, and P_∞ is the stream static pressure, evaluated from the total head and the Mach number. The pressure coefficient c_{pi} was calculated as a function of r/R, r being the distance from the model axis to the pressure tap point at a given section (Fig. 2), and R the distance in the same section from the axis to the edge of the wing. Then a constant value of the variable r/R corresponds to points lying on a single straight line passing through the apex of the model. The results of the calculations at various angles of incidence are shown in Fig. 3. The experimental pressure values on the graph are data from both sections, including also the symmetrically located orifices. The positions of the points indicate that the measured pressures on all the models fit very well on a single line, which confirms the postulate of conical flow in these experiments. It should be noted, however, that there were "drop out" points in the experiments which were not taken into account in constructing the experimental curves; these points appeared in both sections, and are apparently due to non-uniformities of the field or other accidental causes.

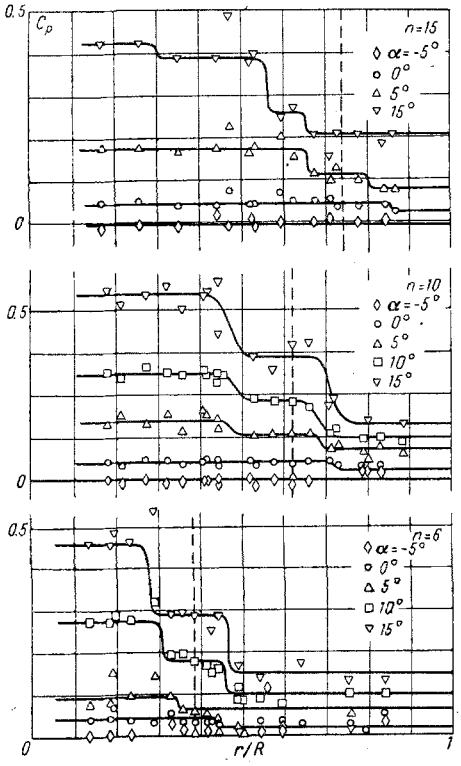

Fig. 3

Let us now proceed to analyze the graphs of pressure distribution shown in Fig. 3 (n = 15). In spite of there being some scatter of the experimental data, the majority of the points decisively indicate that the model surface pressure varies discontinuously, taking different constant values at the separate sections. For instance, the pressure curve at angle of attack $\alpha = 0$ (reference condition) is composed of two parts; the first low-pressure part begins at the wing edge (r/R = = 1) and extends to a point located at a distance ~0.8 from the axis; the second part corresponds to a roughly doubled pressure, and extends from this point to the point where the wings run together. With increase of angle of attack ($\alpha = 5°$) the pressure at all points of the surface increases uniformly, while the shape of the experimental curve remains unchanged and again consists of two constant-pressure parts.

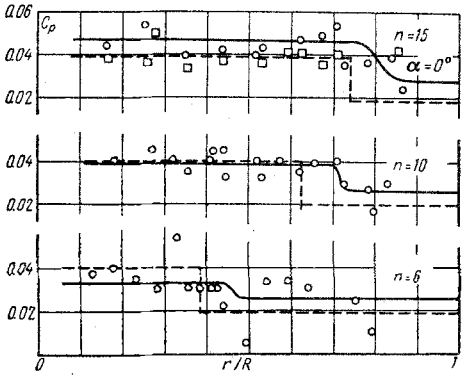

Fig. 4

However, the first reduced-pressure part is elongated, while the second is shortened. At large angles ($\alpha = 15°$), the pressure distribution curve retains its form qualitatively, but the increased-pressure region then breaks down into several constant-pressure levels. The low-pressure part continues to increase, and occupies more and more of the wing surface.

The above findings become comprehensible if we invoke the theoretical picture of the flow and its possible modifications in nonreference conditions ($\alpha \neq \neq 0$). In fact, if the flow at $\alpha = 0$ is close to the reference situation (in the tests the Mach number M_∞ differed from the reference value by 0.1, and the model dimensional errors did not exceed 5%), then the pressure distribution at the wall consists of a section of constant pressure determined by the shock attached to the leading edge, and a region of higher constant pressure arising after the flow passes through the second shock. In the reference condition the second shock is cancelled at the wall (at the break point), and even at small deviations from the reference condition, a secondary reflected shock will evidently appear, detectable on schlieren photographs, but not producing any noticeable pressure increase at the wall. Thus, at small deviations from the reference condition, due to Mach number or incidence angle changes, the shocks intersect regularly, and

the theoretical flow scheme holds. We shall now examine the case of flow at large angle of attack. According to Fig. 3, in this case the incident shocks, and therefore also the reflected shocks, become considerably more intense. Regions of increases pressure now appear, corresponding to reflection of secondary and subsequent shocks. If we trace according to Fig. 3 the variation in position of the first shock reflected from the wall as a function of angle of attack, we note that this point is displaced monotonically within the model. This relation allows us to assume that even at large angles the first shocks intersect regularly, since otherwise the monotonic condition would be disturbed from some point onwards. As far as interaction of the secondary and subsequent shocks is concerned, Mach intersection is not excluded.

The pressure distribution on the remaining two models is qualitatively similar in behavior, but there are appreciable differences for the model with n = 6 at large angle of attack, namely, at $\alpha = 10°$ and 15°, a backward displacement of the point of reflection of the first shock, and a reduced region of constant pressure behind the first shock are observed. The disturbance of the monotonic change of the coordinate of this point with increase of angle of attack, occurring for the other models, most likely denotes transition of the regular intersection of the first shocks to Mach interaction. The more so in that for the range of angles $\alpha = 0°$ to 15° around this model (n = = 6), there are realized the most intense shocks, for which, other conditions being equal, the limiting angle of regular intersection is less than for the other two models. In addition to the cases examined, Fig. 3 also gives graphs of pressure distribution for a negative angle of attack ($\alpha = -5°$). For this condition the pressure at the model surface is practically zero, according to the arrangement of the experimental points. This agrees with the fact that at $\alpha = -5°$ the direction of the oncoming stream roughly coincides with the line of intersection of the wings, and they behave as flat plates aligned with the stream.

It is of interest to compare the experimental pressure distribution with the exact theory [2] for $\alpha = 0$. The theoretical curves are shown as broken lines in Fig. 4, and the average experimental values are the continuous lines. The agreement between experiment and theory on all the graphs may be considered good. The divergence of the data mainly pertains to the dimensions of the increased pressure regions. Going from model to model (n = 15 to n = 6), there is a definite reduction in the difference between theory and experiment. It is natural to suppose that besides the deviations of experimental data from theory arising from model dimensional errors, Mach number departures from the reference value, and other accidental causes, there is some constant factor which increases as n increases. It is most likely that this factor is the boundary layer, which manifests itself more forcibly at larger values of n.

Apropos of this, we should point out that one of the models (n = 15) was tested at zero incidence in another facility at $M_\infty = 3.85$ and substantially greater Reynolds number, $R = 3.6 \cdot 10^7$. The pressure measurement results are shown by the square symbols on Fig. 4 (courtesy of A. I. Zubkov). There is good agreement between the data for the two tunnels, and agreement with theory improves as the Reynolds number increases. Thus the theoretical flow scheme is confirmed both qualitatively and quantitatively by experiment in the range $n \leq 15$.

We also note that in all cases the theoretical solution of [2] containing two weak shocks was compared with experiment. If we assume that one of the shocks is strong, then the data of the theory and experiment differ by a factor of two. We should point out that if we proceed to the limit when $M_\infty \to \infty$ and $\varkappa \to 1$ in the formulas of [2] ($\varkappa$ is the specific heat ratio), we obtain the Newtonian approximation in the case of weak reflected shocks. When the reflected shocks are strong, extra concentrated forces of finite intensity appear at the points where the lobes meet. We may therefore expect that for the star-shaped bodies examined, the Newtonian approximation will prove to be tenable at large Mach numbers. The situation for flow over conical bodies is evidently analogous to the plane case, for which it is known that regular reflection with a weak shock is realized experimentally.

From the pressure distribution data obtained, it is not difficult to calculate the wave drag coefficient of the star-shaped bodies. The experimental values of C_x prove to be 0.029 (n = 6), 0.035 (n = 10), and 0.042 (n = 15). The corresponding theoretical values of C_x are 0.026, 0.029, and 0.032. The ratios of the wave drag of the equivalent circular cone C_x° to that of the star-shaped models tested are as follows: $C_x^\circ/C_x =$ = 3.9 (n = 6), 2.2 (n = 10), 1.95 (n = 15). Thus theory and experiment show good agreement, and a several-fold reduction in wave drag is realized as predicted by theory.

REFERENCES

1. A. L. Gonor, "Three-dimensional bodies with very low drag at high supersonic speeds," PMM, vol. 27, no. 1, 1963.

2. A. L. Gonor, "An exact solution for supersonic flow over certain three-dimensional bodies," PMM, vol. 28, no. 5, 1964.

25 July 1965 Moscow